

Synthesis, characterization and hydrolysis of an aliphatic polycarbonate by terpolymerization of carbon dioxide, propylene oxide and maleic anhydride

Yanfei Liu, Kelong Huang*, Dongming Peng, Hong Wu

Institute of Functional Materials and Chemistry, Central South University, Changsha, Hunan 410083, People's Republic of China

Received 18 April 2006; received in revised form 19 October 2006; accepted 22 October 2006

Available online 9 November 2006

Abstract

Terpolymerization of propylene oxide (PO), carbon dioxide (CO₂) and maleic anhydride (MA) was carried out by using a polymer-supported bimetallic complex (PBM) as a catalyst. A degradable aliphatic poly(propylene carbonate maleate) (PPCM) was synthesized, and determined by FT-IR, ¹H NMR, ¹³C NMR, DSC, TGA and WAXD measurements. The influences of various reaction conditions such as molar ratio of the monomers, reaction time and reaction temperature on the terpolymerization progress were investigated. The results showed that MA was inserted into the backbone of CO₂–PO successfully. The viscosity, glass transition temperature and decomposition temperature of the terpolymers were much higher than those of poly(propylene carbonate) (PPC). Because of the existence of the MA ester unit, PPCM had stronger degradability than PPC in a pH 7.4 phosphate-buffered solution. MA offered an ester structural unit that gave the terpolymers remarkable degradability. And the degradation rate of the backbone increased with the insertion of MA into the terpolymers.

© 2006 Elsevier Ltd. All rights reserved.

Keywords: Aliphatic polycarbonate; Carbon dioxide; Terpolymerization

1. Introduction

Carbon dioxide is currently regarded as an environmental pollutant that causes the greenhouse effect [1–3]. Thus utilization of CO₂ gradually became a topic of intensive study for the sake of environmental concerns and use of this potential carbon resource. One possible utilization approach is to convert the abundant, cheap resources to polymer products [4]. Since the pioneering work of Inoue in 1969 [5], the synthesis of polycarbonates from carbon dioxide and epoxides has been a long-standing interest as a potential way to carbon dioxide utilization [6–10]. In the past decades, most of the researches are focused on how to promote the efficiency of polymerization and activity of catalysts [11–22]. Recently, the work about the modification and applications of polycarbonates has been paid much attention and recognition by researchers

[23–26]. As well as, increasing attention has been paid to the design and synthesis of new copolymers with potential applications as functional materials [27], such as electronic conducting polymers [28], optical polymers [29], biomimetic materials [30], biomedical materials [31–33]. Aliphatic polycarbonates represent one family of biodegradable materials used for biomedical applications such as drug carriers and implant materials because of their good biocompatibility, low toxicity, and biodegradability [34,35]. Synthesis of aliphatic polycarbonates bearing functional groups including alkyl, OH, NH₂, COOH and COOR, is an attractive subject, because these functional groups can be used to regulate the hydrophilicity/hydrophobicity, permeability and mechanical properties [36,37]. The thermal properties and degradability of aliphatic polycarbonates can also be improved by introducing the third monomer into the copolymerization of carbon dioxide and propylene oxide. In our work group, two kinds of terpolymers have been synthesized by terpolymerization, they showed remarkable degradability than PPC [38–40]. Their application as drug carriers has also been investigated [40]. In the present

* Corresponding author. Tel./fax: +86 731 8879850.

E-mail address: kelonghuang@yahoo.com.cn (K. Huang).

work, another polycarbonate (PPCM) was successfully synthesized with the third monomer MA, and PBM used as catalyst to ensure the terpolymerization of CO₂, PO and MA. The ring-opened MA units were found to be linked to the propylene carbonates directly and no blocked MA was detected, the copolymers had amorphous structure. The novel aliphatic carbonates showed high glass transition temperatures and good degradability.

2. Experimental

2.1. Materials

PO (Shanghai Chemical Reagents Co., A.R. grade) and toluene (Hengyang Organic Chemical Reagents Plant, A.R. grade) were dehydrated by 0.4 nm molecular sieves prior to use. MA (A.R. grade) was purchased from Shantou Xilong Chemical Factory, Guangdong. CO₂ and N₂ (purity more than 99.5%) were purchased from Hunan Special Gas Factory (China). All other reagents and solvents were of analytical grade and used without further purification.

2.2. Preparation of catalyst

The P–Zn[Fe(CN)₆]_aCl_{2–3a}(H₂O)_b (PBM) was used as a catalyst for the copolymerization of CO₂ and relevant comonomers, and was synthesized according to the literature [41]. For example, ZnCl₂ (2.436 g) and poly(ethylene glycol) (*M*_w 600) (36.974 g) were mixed in a 500 ml beaker. K₃Fe(CN)₆ (1.646 g) was dissolved in distilled water. Both reagents were mixed under vigorous stirring and the precipitate was filtered, collected, washed with distilled water, and dried under vacuum till constant weight. The resulting fine yellow powder was then stored until use.

2.3. Preparation and purification of copolymers

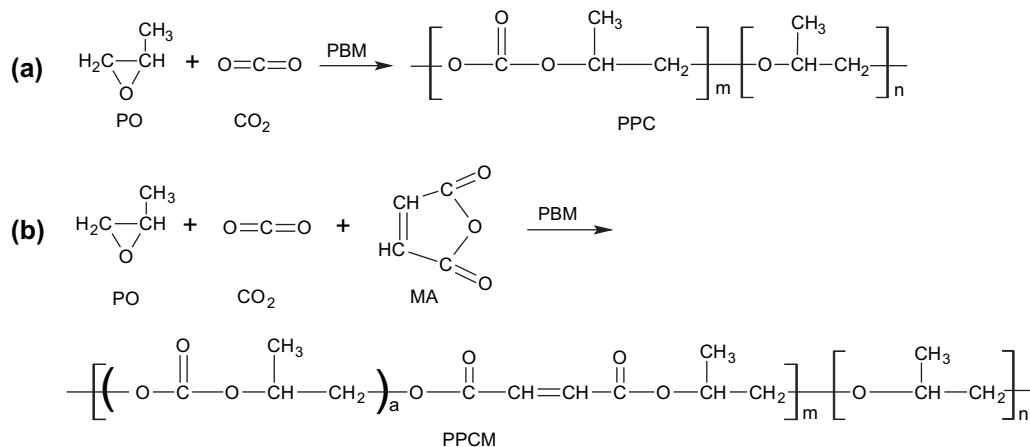
The preparations of the copolymers, poly[(propylene oxide)-*co*-(carbon dioxide)] (PPC) and poly[(propylene oxide)-

co-(carbon dioxide)-*co*-(maleic anhydride)] (PPCM), were carried out in a 300 ml stainless steel autoclave equipped with a magnetic stirrer. They were synthesized in similar procedure and both reactions are shown in Scheme 1.

The reactor was connected to dry nitrogen and CO₂ cylinder using a three-way valve. Required amount of catalyst, solvents and other solids or liquid reagents was added into the autoclave in the absence of oxygen. The autoclave was then pressurized to 3.5–4 MPa with a CO₂ cylinder. The reaction mixture was stirred magnetically at desired temperature for a certain period. When the reaction was finished, the reactor was cooled to room temperature, and the pressure was released. The resulting viscous mixture was collected after toluene and excess PO were evacuated. The mixture was then washed with C₂H₅OH, which contained 5% HCl, and three times with only C₂H₅OH. The precipitate was dried in a vacuum drying oven. For purification, the dried copolymer was dissolved in CH₂Cl₂. The product solution was filtered to remove the residual catalyst. Finally, it was precipitated by being poured into vigorously stirred methanol. The methanol-insoluble product was centrifuged, collected and dried under vacuum at a temperature of 30 °C until a constant weight was obtained.

2.4. Hydrolytic degradation

These copolymers were insoluble in water; the hydrolysis tests were carried out to appraise the copolymers' degradability. The copolymers were dissolved in CH₂Cl₂ to make 8 wt% solutions and formed films of about 1 mm thickness on polytetrafluoroethylene templates after the volatilization of the solvent. The films were dried under vacuum at 35 °C to a constant weight, then immersed in vials filled with a phosphate-buffered saline solution (PBS, 0.1 M, pH 7.4), and placed in a thermostat for various periods at 37 °C. Samples were recovered weekly, the mass loss and the water uptake of the samples were determined by gravimetric analysis, while changes of molecular weight were measured. The surface morphological changes of copolymer films were monitored by scanning



Scheme 1. (a) Copolymerization of carbon dioxide with propylene oxide. (b) Terpolymerization of carbon dioxide with propylene oxide and maleic anhydride.

electron microscope. The degradability of the copolymers was determined through total weight loss of these samples over a certain time. The type of erosion was evaluated by changes in molecular weight.

2.5. Characterization

FT-IR spectra were recorded on Nicolet AVATAR360 FT-IR spectrometer. ^1H NMR and ^{13}C NMR spectra were recorded at 300 MHz on a Varian Inova-300 spectrometer with CDCl_3 as solvent. The molar fractions of CO_2 , PO and MA were calculated by integrating the areas. The glass transition temperature (T_g) of the copolymers was determined by differential scanning calorimetry (DSC) on a TA DSC-Q10 instrument; the samples were heated in two cycles from -10°C to 80°C at a rate of $10^\circ\text{C}/\text{min}$ in nitrogen atmosphere. T_g of the samples was determined from the second run. The decomposition process of the polymers from 50°C to 500°C was determined with a Setaram Labsys thermogravimetric analyzer under a protective nitrogen atmosphere. The heating rate employed was $10^\circ\text{C}/\text{min}$. The surface morphologies of copolymer films were taken by a scanning electron microscope (KYKY2800, China). Intrinsic viscosity $[\eta]$ measurements were carried out in benzene at $35 \pm 0.1^\circ\text{C}$ using an Ubbelohde suspended level capillary viscometer. The molecular weight was calculated from the equation $([\eta] = 1.11 \times 10^{-4} [M_n]^{0.8} \text{ (dL/g)})$ [42]. The wide-angle X-ray diffraction (WXR) measurements were performed at room temperature using a Rigaku D/max 2550 VB⁺ 18 Kw X-ray diffractometer to analyze the structure. Elemental analysis was carried out on an Elementar Vario EL III instrument.

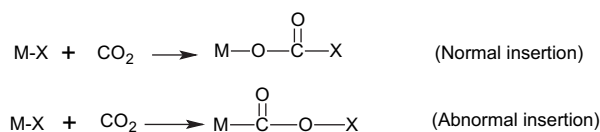
3. Results and discussion

3.1. Expected mechanism of terpolymerization

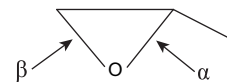
CO_2 is highly thermodynamically stable and kinetically inert, so an increased use of CO_2 would only be possible if the relatively inert CO_2 molecule could be activated [43]. As a monomer, CO_2 requires for its copolymerization large amounts of anionic coordination catalysts [44], such as $\text{ZnEt}_2/\text{H}_2\text{O}$, $\text{ZnEt}_2/\text{multihydric alcohols}$ or carboxylic acids, zinc glutarate, and metalloporphyrin complexes. Applications of certain bimetallic combination and some polymeric chelating ligands were found to be very effective in improving the catalytic activity. Thus a type of polymer-supported bimetallic complexes (PBM) in the form of $\text{P-Zn}[\text{Fe}(\text{CN})_6]_a\text{Cl}_{2-3a}(\text{H}_2\text{O})_b$ were developed, where P is polyether type chelating agent, $a \approx 0.5$ and $b \approx 0.76$. PBM is a yellow powder, does not dissolve in water and organic solvents, is stable to air, and can be handled and stored easily. CO_2 can be activated to a high extent by using macromolecule–metal complexes, PBM has been known to be effective catalyst to produce aliphatic polycarbonates with a nearly alternating structure [41]. Terpolymerization of CO_2 with epoxide and cyclic anhydride belongs to anionic coordination polymerizations. The accepted mechanism of this reaction is anionic coordinate-

insertion mechanism, similar to the previously reported literature [21,44]. An anionic mechanism for the terpolymerization of CO_2 , PO and MA is proposed here as follows. Zinc is the active metal center of the complexes for the coupling of CO_2 and comonomers. Firstly, CO_2 is activated by the coordination to the active sites of $\text{Zn}(\text{II})$ centers, and then is inserted into the M-X bond of catalyst, activating the zinc metal center. In the next step, PO and MA interact with the activated zinc metal center and are inserted into the growing chain, alternately. Then, the copolymerization is considered to proceed via the alternating repetition of additions of CO_2 , PO and MA to the active terminal of the growing polymer, on the other hand, when the reactions of epoxide take place repeatedly, ether bonds are formed, in addition to carbonate linkages in the polymer main chain. As a result, the obtained copolymer contains both carbonate and ether linkages.

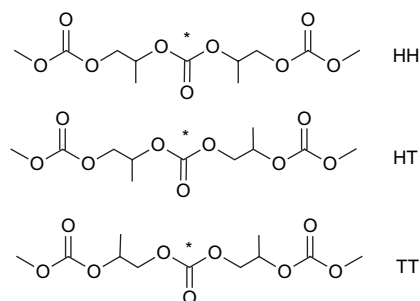
CO_2 and MA could not homopolymerize nor copolymerize under the reaction conditions. Thus the terpolymerization involves competitive alternating copolymerization of PO with CO_2 , PO with MA, and homopolymerization of PO. As shown in Scheme 2, there are two possible modes of CO_2 insertion into the M-X bond of catalyst; normal insertion leads to the formation of a carboxylate complex [43]. The ring opening of epoxide is typically favored at the least-hindered C–O bond, although cleavage is normally observed at both. As shown in Scheme 3, propylene oxide has one asymmetric carbon atom; β opening is accompanied by α opening during the coupling reaction and the selective incorporation of propylene oxide monomer is a determining factor to influence the microstructure of the copolymer. As shown in Scheme 4, there usually exist tail-to-tail (T–T), head-to-head (H–H) and



Scheme 2. The way of carbon dioxide insertion into M-X bond.



Scheme 3. Bond cleavage of propylene oxide in the copolymerization of CO_2 and epoxide.



Scheme 4. Regiosequence of carbonate unit and ether unit.

head-to-tail (H–T) carbonate groups in the copolymers, H–T unit is dominant [20,45]. The expected mechanism is illustrated in Scheme 5. The proposed structure of the resulting terpolymer can be seen in Scheme 1.

3.2. Structural characterization of copolymers

PPC and PPCM53 were used as samples for the FT-IR, WXR, ^1H NMR and ^{13}C NMR characterization.

The FT-IR spectra of PPC and PPCM53 are shown in Fig. 1. The copolymer of PPCM had characteristic FT-IR absorptions at 1740 cm^{-1} (s, C=O), 1236 cm^{-1} (s, C–O), 788 cm^{-1} and 1070 cm^{-1} (s, C–O–C), and they were similar to those of PPC. Otherwise, the asterisk-marked peak in the FT-IR spectra of PPCM at 1645 cm^{-1} was found to be responsible for the C=C vibration, indicating that MA was inserted into copolymer chain.

The ^1H NMR spectra of PPC are shown in Fig. 2(a). The ^1H NMR spectra confirmed the existence of carbonate link: ^1H NMR (δ , CDCl_3), δ 1.34 (d, CH_3), 5.0 (m, $\text{CH}(\text{CO}_3)$), 4.2 (m, $\text{CH}_2(\text{CO}_3)$). The signals at 3.5 ppm and 1.2 ppm were assigned to the hydrogen in ether linkage of propylene oxide. The signal at 7.26 ppm was assigned to CDCl_3 . The characteristic proton chemical shifts of carbonate link and ether link of propylene oxide were also observed in the ^1H NMR spectra of PPCM (Fig. 3(a)): δ 1.34 [3H, CH_3 (a)], 5.0 [1H, $\text{CH}(\text{CO}_3)$ (b)], 4.2 [2H, $\text{CH}_2(\text{CO}_3)$ (c)], 1.2 [3H, CH_3 (a')], 3.5 [3H, $\text{CH}_2\text{CH}(b',c')$]; there was another proton chemical shift at δ 6.3 [2H, $\text{CH}=\text{CH}(d,e)$], indicating that the content of the MA unit, which was inserted into the backbone of CO_2 –PO.

The ^{13}C NMR spectra of PPC and PPCM53 are shown in Figs. 2(b) and 3(b), respectively. The main signals for PPC were assigned as follows: δ 153–155 (CO_3), 72.3 (CH-O), 70.5 (CH_2), 16.2 (CH_3), and 77.0 (CDCl_3). The signals for PPCM53 were assigned as follows: δ 153–155 [OCOO(A)], 72.3 [CH(B)], 70.5 [$\text{CH}_2(\text{C})$], 16.0 [$\text{CH}_3(\text{D})$], 128–130 [$\text{CH}=\text{CH}(\text{E,F})$], 165 [COO(G)], and 73.7 [CH(B')], 72.1 [$\text{CH}_2(\text{C'})$], 16.3 [$\text{CH}_3(\text{D'})$]. According to the literatures reported previously [46,47], T–T, H–T, and H–H carbonate

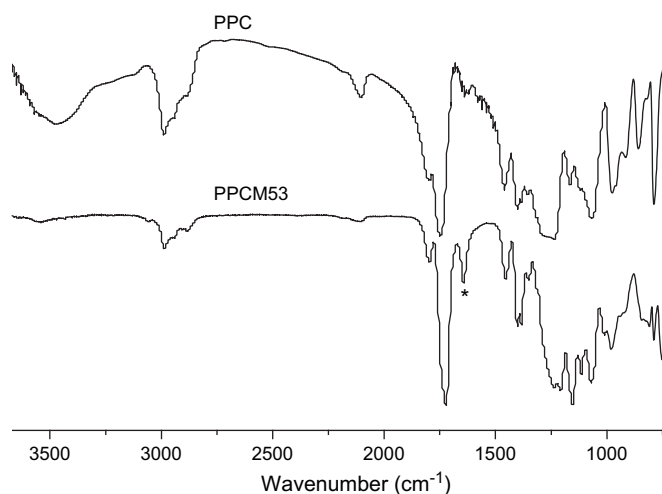


Fig. 1. FT-IR spectra of PPC and PPCM53.

groups correspond to the signals located at 154.8 ppm, 154.2 ppm and 153.6–153.8 ppm in the ^{13}C NMR spectra, respectively. Carbonate carbon signals of PPC and PPCM were magnified and shown in Figs. 2(b) and 3(b), the values reveal that H–T junctions are predominant in both PPC and PPCM.

The FT-IR, ^1H NMR and ^{13}C NMR spectra confirmed that MA was ring-opened and inserted into the backbone of CO_2 –PO successfully.

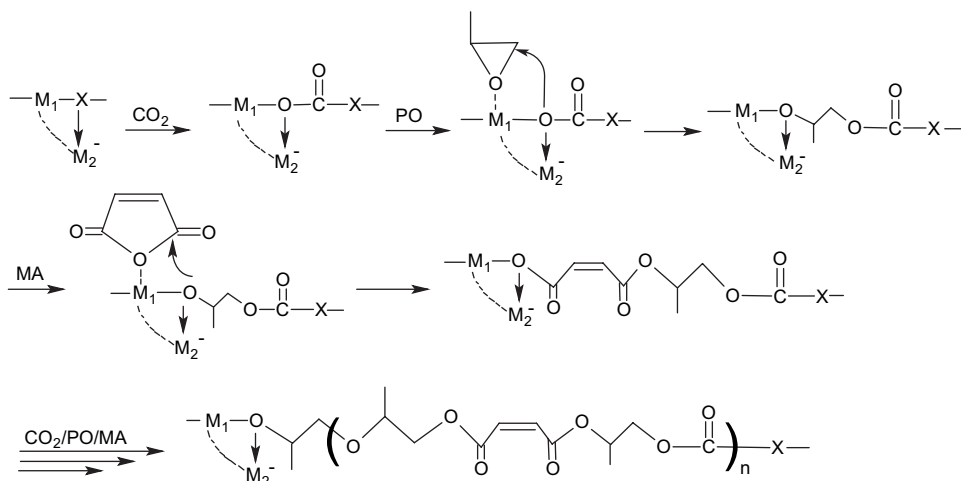
According to the integration of the ^1H NMR spectra of the copolymers, the composition of copolymer was calculated by the following equations:

$$f_{\text{PO}} = (A_{5.0} + A_{4.2} + A_{3.5}) / [2(A_{5.0} + A_{4.2}) + A_{3.5}]$$

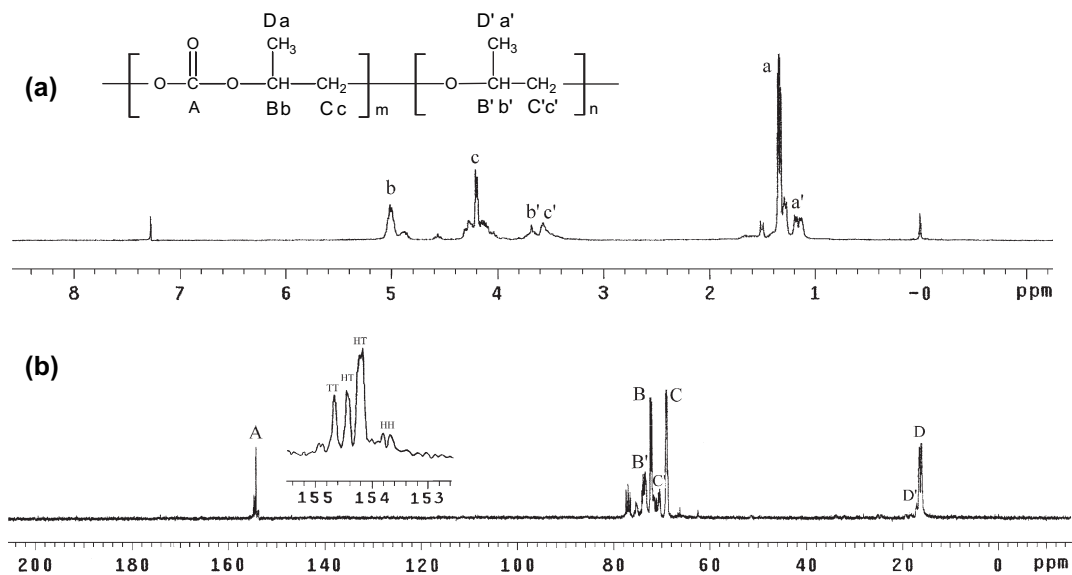
$$f_{\text{MA}} = \frac{3}{2} A_{6.3} / [2(A_{5.0} + A_{4.2}) + A_{3.5}]$$

$$f_{\text{CO}_2} = 1 - f_{\text{PO}} - f_{\text{MA}}$$

As shown in Table 1, the molar fractions of CO_2 (f_{CO_2}) in PPC were 42.67%, while f_{CO_2} in PPCM terpolymers were



Scheme 5. The expected mechanism of CO_2 –PO–MA copolymerization. $\text{M}_1 = \text{Zn}$, $\text{M}_2 = \text{Fe}$, $\text{X} = \text{Cl}$.

Fig. 2. ^1H NMR (a) and ^{13}C NMR (b) spectra of PPC.

lower than that. The decrease of f_{CO_2} was due to the introduction of the third monomer into the backbone. As the amount of MA fed into the reactions increased, the molar fractions of MA (f_{MA}) increased. The value of f_{MA} was 27.82% when PO:CL ratio reached 5:3. However, as the PO:MA ratio went beyond 5:3, f_{MA} increased very slightly tending to remain constant. It was considered that the transformation efficiency was high when the amount of MA fed into the reactions was not very large. But as the MA content went on increasing, the amount of dissociative MA increased, excess MA would

surround the active centers and prevent PO from contacting with the active centers. In addition, MA and CO_2 could not copolymerize under the reaction conditions. Thus, excess MA hampered the reactions and resulted in the slight increase of f_{MA} . The elemental analysis data for PPC and PPCM are listed in Table 1. The results revealed that the calculated data of elemental contents were close to the found data; the differences were not significant.

The wide-angle X-ray diffraction spectra (Fig. 4) indicate that the terpolymers were amorphous, and there was no MA

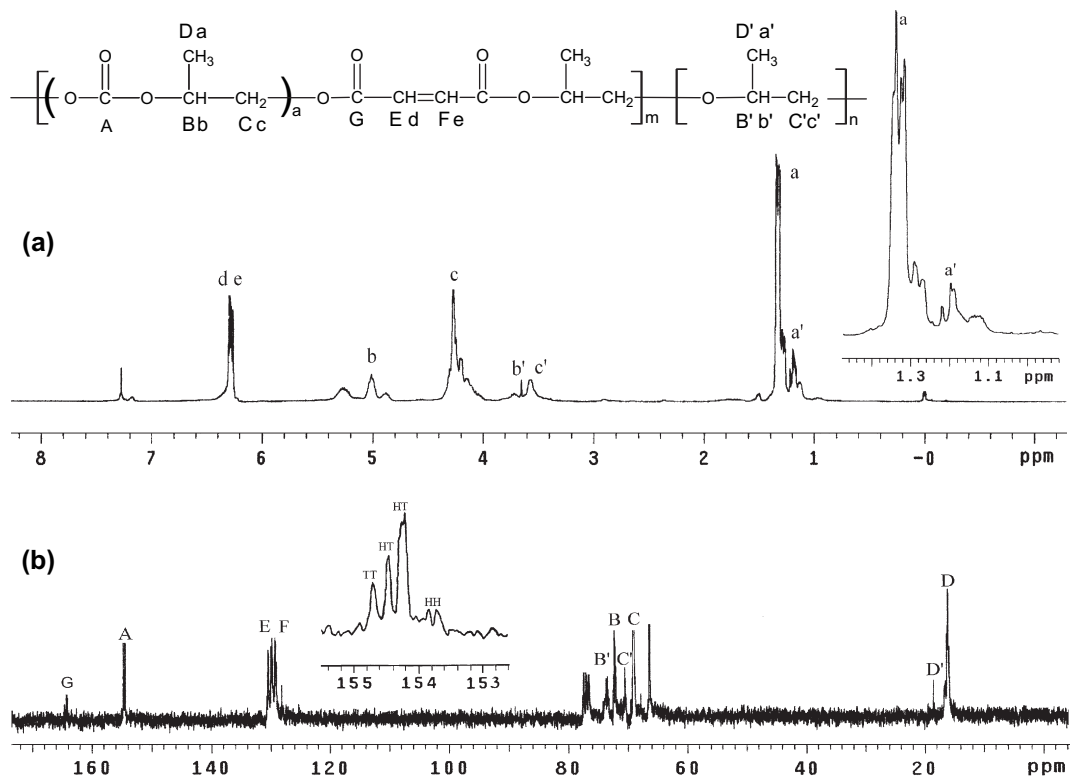
Fig. 3. ^1H NMR (a) and ^{13}C NMR (b) spectra of PPCM53.

Table 1
Influence of PO:MA molar ratio on composition of the copolymers

Copolymer	PO:MA (molar ratio)	Composition ^a (molar fraction in %)			Elemental analysis (%)			
		f_{CO_2}	f_{PO}	f_{MA}	C	H	O	
PPC	5:0	42.67	57.33	0.00	Calcd	49.5	6.6	43.9
					Found	48.7	6.6	44.7
PPCM51	5:1	33.15	55.39	11.46	Calcd	50.8	6.1	43.1
					Found	50.6	6.4	43.0
PPCM52	5:2	25.91	53.60	20.49	Calcd	51.5	5.8	42.7
					Found	51.2	6.1	42.7
PPCM53	5:3	19.39	52.79	27.82	Calcd	51.9	5.6	42.5
					Found	51.7	5.9	42.4
PPCM54	5:4	19.08	52.14	28.78	Calcd	52.2	5.5	42.3
					Found	52.2	5.7	42.1
PPCM55	5:5	18.69	51.86	29.45	Calcd	52.2	5.5	42.3
					Found	52.4	5.5	42.1

Reaction conditions: $T = 60\text{ }^\circ\text{C}$; $t = 24\text{ h}$.

^a The molar fractions of CO_2 , PO and MA calculated by integrating areas of ^1H NMR spectra of PPC and PPCM.

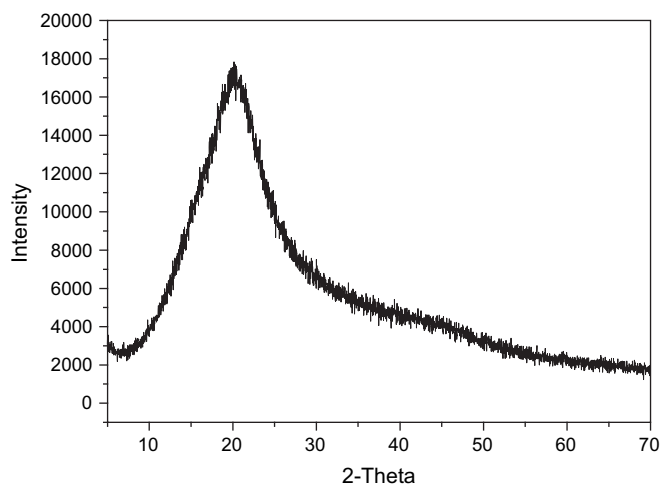


Fig. 4. The wide-angle X-ray diffraction spectra of PPCM53.

homopolymer or blocked MA in the products. The DSC curves of PPCM polymers (Figs. 5 and 6) revealed only a single T_g and no crystalline melting point also confirmed that.

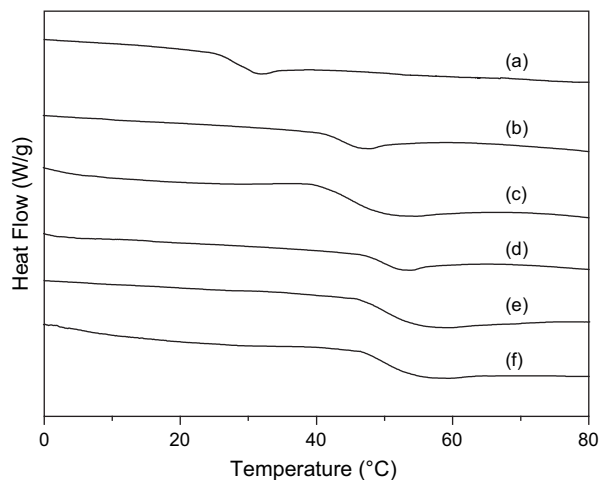


Fig. 5. DSC curves of terpolymers prepared from different PO:MA molar ratio. (a) PPC; (b) PPCM51; (c) PPCM52; (d) PPCM53; (e) PPCM54; (f) PPCM55.

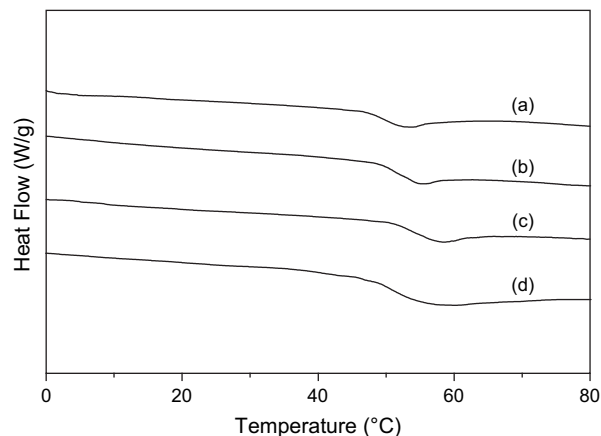


Fig. 6. DSC curves of terpolymers prepared from different reaction times. (a) 24 h; (b) 36 h; (c) 48 h; (d) 60 h.

All of the experimental results, such as microstructural analysis, are in agreement with the expected mechanism.

3.3. Influence of PO:MA molar ratio

Table 2 shows the influence of PO:MA molar ratio on the properties of the terpolymers. The $[\eta]$ and M_v are all related to the structure and components of the terpolymers, they increased with increasing MA content. The T_g of the PPCM

Table 2
Influence of PO:MA molar ratio on terpolymerization

Copolymer	PO:MA (mol:mol)	Yield ^a (g/g of cata.)	$[\eta]$ (dL/g)	M_v ($\times 10^4$)	T_g ($^\circ\text{C}$)
PPC	5:0	36.02	0.515	3.83	29.1
PPCM51	5:1	36.93	0.590	4.54	43.6
PPCM52	5:2	44.18	0.683	5.45	45.7
PPCM53	5:3	49.38	0.772	6.35	49.8
PPCM54	5:4	41.66	0.826	6.91	50.7
PPCM55	5:5	40.15	0.855	7.22	51.6

Reaction conditions: $T = 60\text{ }^\circ\text{C}$; $t = 24\text{ h}$; 0.5 mol PO; 1.0 g catalyst.

^a Yield of copolymer insoluble in methanol.

terpolymers was higher than that of PPC, and increased with increasing M_v .

3.4. Influences of reaction time

The influence of reaction time on T_g , $[\eta]$ and M_v is shown in Table 3. The longer the reaction time was, the higher the $[\eta]$, M_v and T_g of the terpolymers was. However, when the reaction time was prolonged to 60 h, both $[\eta]$ and T_g declined. It was found that the relation between the molecular weight and reaction time accorded with the mechanism of anionic coordination polymerization. It was explained as that the terpolymerization had a certain induction period. The velocity of the reaction was speeded up after the induction period. At the same time the heat was released and the molecular weight reached a maximum value. However, as the reaction time was over-prolonged, the velocities of chain transfer and decomposition would go beyond the normal value, and resulted in the decline of $[\eta]$ and M_v .

3.5. Influences of reaction temperature

The influence of reaction temperature on the terpolymerization was investigated with temperature change from 50 °C to 80 °C. The results are summarized in Table 4. At 50 °C, the $[\eta]$ of the resulting polymer was only 0.567 dL/g. The intrinsic viscosity increased as the reaction temperature changed from 50 °C to 70 °C and it had maximum value at 70 °C. Then the intrinsic viscosity dropped rapidly when the temperature was increased from 70 °C to 80 °C. That is because higher temperature was a benefit to reduce the induction period and accelerate the reaction speed. However, when the temperature was higher than 70 °C, increasing the reaction temperature accelerated the copolymerization as well as the chain transfer

Table 3
Influence of reaction time on terpolymerization

Copolymer	Reaction time (h)	Yield ^a (g/g of cata.)	$[\eta]$ (dL/g)	M_v ($\times 10^4$)	T_g (°C)
PPCM24	24	49.38	0.722	6.35	49.8
PPCM36	36	49.89	0.861	7.28	52.1
PPCM48	48	50.64	0.911	7.81	53.4
PPCM60	60	47.81	0.838	7.04	51.5

Reaction conditions: $T = 60$ °C; 0.5 mol PO; PO:MA ratio = 5:3; 1.0 g catalyst.

^a Yield of copolymer insoluble in methanol.

Table 4
Influence of reaction temperature on terpolymerization

Copolymer	Reaction temperature (°C)	Yield ^a (g/g of cata.)	$[\eta]$ (dL/g)	M_v ($\times 10^4$)
PPCM (a)	50	32.08	0.567	4.32
PPCM (b)	60	49.38	0.772	6.35
PPCM (c)	70	50.08	0.787	6.51
PPCM (d)	80	42.21	0.364	2.48

Reaction conditions: $t = 24$ h; 0.5 mol PO; PO:MA ratio = 5:3; 1.0 g catalyst.

^a Yield of copolymer insoluble in methanol.

and depolymerization, thus resulting in the decline of intrinsic viscosity and molecular weight. The optimal terpolymerization temperature was between 60 °C and 70 °C.

3.6. Hydrolytic degradation

Hydrolytic degradation is caused by the reaction of water with labile bonds, typically ester bonds, in the polymer chain [48]. Polymer erosion was monitored by following mass loss, water uptake, molecular weight changes, and surface morphology. The degradability of the terpolymers synthesized from various PO:MA ratios was determined in order to discover the influence of MA on degradability. It can be seen from Fig. 7 that PPCM55 had the best degradability which contained the most molar fraction of MA (29.45%). The higher the molar fraction of MA, the higher the hydrolytic activity was. However, the hydrolytic rate did not obviously increase when the molar ratio of PO:MA was up to 5:3. This may be interpreted as follows: although the MA content in the feed increased sequentially when the ratio of PO:MA reached 5:3, the molar ratio of PO and MA monomers in the resulting copolymers still remained at about 5:3. Therefore, the redundant MA was not to be added to the polymerization. This was in accordance with the elemental analysis and the structural unit molar fractions of the copolymers listed in Table 1. The data indicate that the hydrolytic activity of PPCM is much stronger than PPC. This could be due to the introduction of the hydrolytic ester units that are in MA. The water uptake of the samples at various degradation stages was low, that of PPC did not exceed 4%, and of PPCM was less than 8%. During degradation, the molecular weight of the recovered samples decreased very slightly with degradation time. As shown in Fig. 8, after degradation for 8 weeks, M_v of PPCM53 was decreased 14.65% of its initial molecular weight, and PPC was decreased 7.83%. It is well known that the morphological changes of polymer surface can provide direct information for their degradation characteristics. As shown in Fig. 9, the surface of PPCM53 before

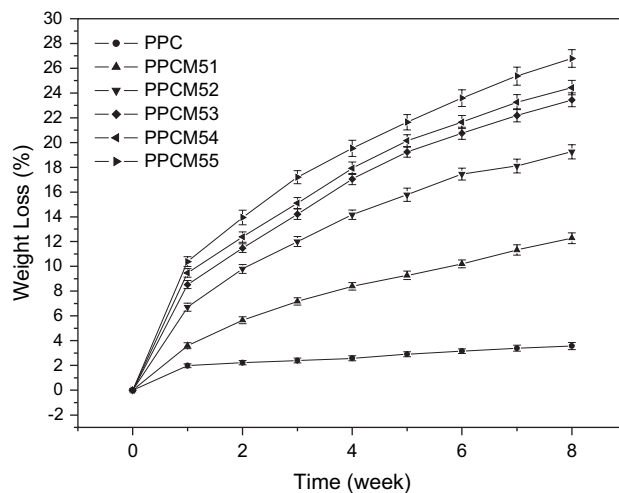


Fig. 7. Influence of PO:MA ratio on the degradability of PPCM. Results given are the mean \pm SD of three independent experiments.

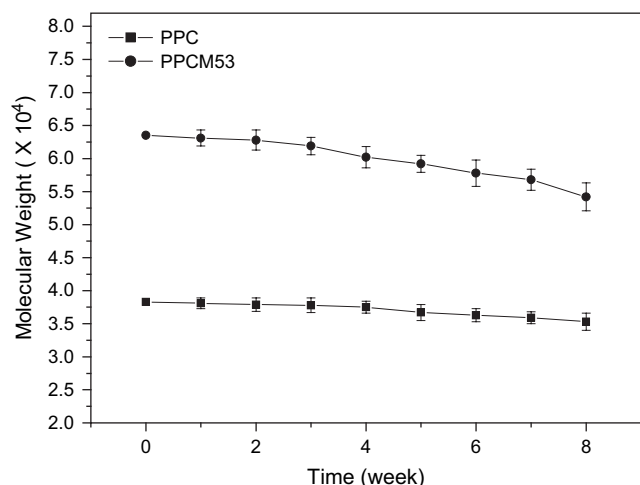


Fig. 8. Molecular weight variation of PPC and PPCM53 during degradation. Error bars indicate standard deviation.

degradation was smooth, and after degradation in the buffer solution for 6 weeks, number of micropores can be observed in the samples, evincing that the degradation begins from the surface, and where degradation favors further degradation, therefore, produces micropores in the surface of films.

The degradation and erosion of polymers are complicated; we supposed that the process of PPCM was as follows: water

penetrated into the polymer matrix, and hydrolytic degradation was caused by the reaction of water with ester bonds in the polymer chain, which induced chain scission to form oligomers and monomers. Progressive degradation changed the microstructure of the bulk through the formation of pores, via which oligomers and monomers were released, leading to the weight loss of polymer films. The water uptake of the copolymers was low, thus the water penetration was slow compared to the erosion process, and mass loss was confined to the surface layers of the samples. The degradation products were diffused to the degradation medium before measuring the molecular weight, so the molecular weight of the copolymers changed slightly. Therefore, we infer that the degradation mainly occurs on the surface of PPCM.

3.7. Thermal degradation

The decomposition temperature (T_d) was determined by thermogravimetric analysis. Fig. 10(a) and (b) shows the TGA–DTG curves of PPC and PPCM53, respectively. The 5% weight-loss temperatures ($T_{d5\%}$) and the maximum weight-loss temperatures (T_{dmax}) of PPC are 200 °C and 238 °C, and those of PPCM are 216 °C and 312 °C, respectively. The results indicated that the introduction of MA into copolymerization can improve the thermal properties, PPCM was found to be more thermally stable than PPC.

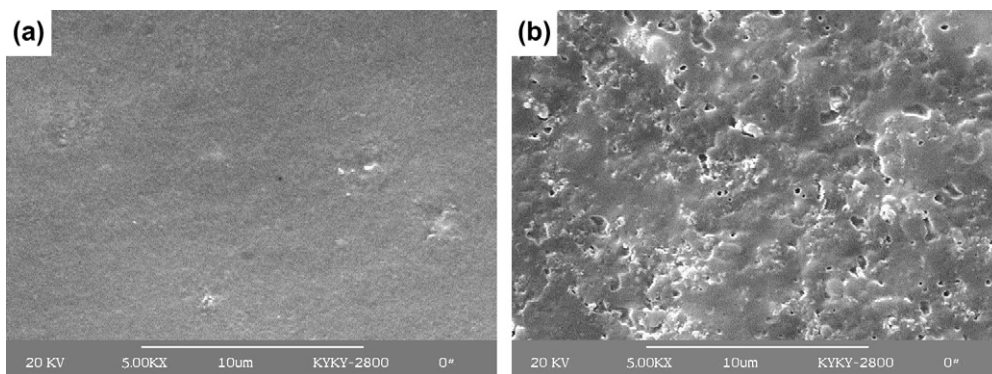


Fig. 9. SEM micrographs of PPCM53 films: (a) before degradation; (b) after hydrolytic degradation in PBS (pH = 7.4) for 6 weeks.

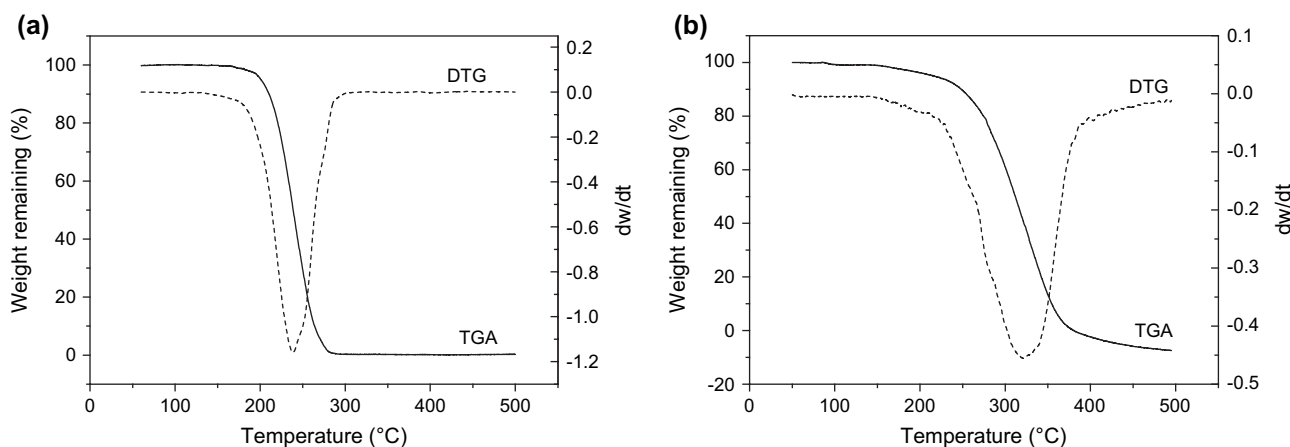


Fig. 10. The TGA–DTG curves of (a) PPC and (b) PPCM53.

4. Conclusion

PPCM terpolymerized from CO₂, PO and MA was successfully synthesized using polymer-supported bimetallic complex (PBM) as a catalyst. As the third monomer, MA had a positive influence on improving the $[\eta]$ and M_v . The thermal properties of PPC were improved via introduction of MA during copolymerization. $T_{d5\%}$ of PPCM53 was 200 °C, that of PPC was 216 °C. The T_g of PPCM48 was as high as 53.4 °C, while that of PPC was only 29.1 °C. The PPCM terpolymers showed remarkable degradability. The weight loss of PPCM55 was 26.78% after degradation in PBS (pH = 7.4) for 8 weeks. In contrast, PPC itself exhibited a very tiny weight loss. These results indicate that the terpolymerization is an effective means to generate a copolymer with the desired degradability and thermal properties; the terpolymer PPCM is a potential material for controlled drug delivery and in other fields requiring degradable materials.

Acknowledgements

Financial support from National High Technology and Development Research ‘863’ Program of China (2001AA218011) is gratefully acknowledged.

References

- [1] Broecker WS. *Science* 1997;278:1582–8.
- [2] Meehl GA, Washington WM. *Nature* 1996;382:56–60.
- [3] Santer BD, Taylor KE, Wigley TML, Johns TC, Jones PD, Karoly DJ, et al. *Nature* 1996;382:39–46.
- [4] Beckman EJ. *Science* 1999;283:946–7.
- [5] Inoue S, Tsuruta T, Koinuma H. *J Polym Sci Polym Lett* 1969;B7:287–92.
- [6] Kruper WJ, Swart DJ. US Patent 4,500,704; 1985.
- [7] Koinuma H, Hirai H. *Makromol Chem* 1997;178:1283–8.
- [8] Zhu Q, Meng YZ, Tjong SC. *Polym Int* 2002;51:1079–85.
- [9] Lee B, Jung JH, Ree M. *Macromol Chem Phys* 2000;201:831–9.
- [10] Zhu Q, Meng YZ, Tjong SC, Zhang YM, Wan W. *Polym Int* 2003;52:799–804.
- [11] Soga K, Uenishi K, Hosoda S, Ikeda S. *Makromol Chem* 1977;178:893–7.
- [12] Soga K, Hyakkoku K, Ikeda S. *J Polym Sci Polym Chem Ed* 1979;17:2173–80.
- [13] Chen X, Shen Z, Zhang Y. *Macromolecules* 1991;24:5305–8.
- [14] Tan C, Hsu T. *Macromolecules* 1997;30:3147–50.
- [15] Super M, Berluche E, Costello C, Bechman E. *Macromolecules* 1997;30:368–72.
- [16] Ree M, Bae JY, Jung JH, Shin TJ. *J Polym Sci Part A Polym Chem* 1999;37:1863–76.
- [17] Ree M, Bae JY, Jung JH, Shin TJ, Huang YT, Chang T. *Polym Eng Sci* 2000;40:1542–52.
- [18] Darensbourg DJ, Yarbrough JC. *J Am Chem Soc* 2002;124:6335–42.
- [19] Takeuchi D, Sakaguchi Y, Osakada K. *J Polym Sci Part A Polym Chem* 2002;40:4530–7.
- [20] Quan Z, Wang W, Zhao X, Wang F. *Polymer* 2003;44:5605–10.
- [21] Chen S, Hua ZJ, Fang Z, Qi GR. *Polymer* 2004;45:6519–24.
- [22] Wang JT, Shu D, Xiao M, Meng YZ. *J Appl Polym Sci* 2006;99:200–6.
- [23] Takanashi M, Noruma Y, Yoshida Y, Inoue S. *Makromol Chem* 1982;183:2085–92.
- [24] Yang SY, Fang XG, Chen LB. *Polym Adv Technol* 1996;7:605–8.
- [25] Hwang Y, Jung J, Ree M. *Macromolecules* 2003;36:8210–2.
- [26] Hwang Y, Kim H, Ree M. *Macromol Symp* 2005;224:227–38.
- [27] Grubbs RH, Friend RH, Meijer EW, Richards RW, Cameron NR. *Polymer* 2005;46:1427–38.
- [28] Plesse C, Vidal F, Randriamahazaka H, Teyssié D, Chevrot C. *Polymer* 2005;46:7771–8.
- [29] Li Z, Gong W, Qin JG, Yang Z, Ye C. *Polymer* 2005;46:4971–8.
- [30] Jiang GH, Wang L, Yu HJ, Chen C, Dong XC, Chen T, et al. *Polymer* 2006;47:12–7.
- [31] Jiang GH, Wang L, Chen T, Yu HJ, Dong XC, Chen C. *Polymer* 2005;46:9501–7.
- [32] Yuan WZ, Tang XZ, Huang XB, Zheng SX. *Polymer* 2005;46:1701–7.
- [33] Açikses A, Kaya I, Sezek Ü, Kirilmis C. *Polymer* 2005;46:11322–9.
- [34] Zhu KJ, Hendren RW, Jensen K, Pitt CG. *Macromolecules* 1991;24:1736–40.
- [35] Rokicki G. *Prog Polym Sci* 2000;25:259–342.
- [36] Mullen BD, Tang CN, Storey RF. *J Polym Sci Part A Polym Chem* 2003;41:1978–91.
- [37] Liu ZL, Zhou Y, Zhuo RX. *J Polym Sci Part A Polym Chem* 2003;41:4001–6.
- [38] Lu LB, Huang KL. *Polym Int* 2005;54:870–4.
- [39] Liu SQ, Xiao H, Huang KL, Lu LB, Huang QY. *Polym Bull* 2006;56:53–62.
- [40] Lu LB, Huang KL. *J Polym Sci Part A Polym Chem* 2005;43:2468–75.
- [41] Chen LB. *Makromol Chem Macromol Symp* 1992;59:75–81.
- [42] Quan Z, Min J, Zhou Q, Xie D, Liu J, Wang S, et al. *Macromol Symp* 2003;195:281–6.
- [43] Yin XL, Moss JR. *Coord Chem Rev* 1999;181:27–59.
- [44] Rokicki A, Kuran W. *J Macromol Sci Rev Macromol Chem* 1981;21:135–41.
- [45] Darensbourg Donald J, Matthew W. *Coord Chem Rev* 1996;181:27–59.
- [46] Lednor PW, Rol NC. *J Chem Soc Chem Commun* 1985;9:598–9.
- [47] Chisholm MH, Navarro-Liobet D, Zhou Z. *Macromolecules* 2002;35:6495–504.
- [48] Edlund U, Albertsson AC. *Adv Polym Sci* 2001;157:67–112.